Direct Instantaneous Torque Controlled Switched Reluctance Motor Drive for Fan Type Load and Constant Torque Load

Srinivas Pratapgiri

Additional information is available at the end of the chapter

Abstract

Switched reluctance motor (SRM) drives can be a good competitor to conventional induction and permanent magnet motors in variable speed applications because of advantages, such as simple construction, no rotor windings, high torque to inertia ratio, adaptability to hostile conditions, etc. Due to its high nonlinearity, the torque ripple is high in switched reluctance motor. The sophisticated direct instantaneous torque control (DITC) can maintain the torque developed by the motor within hysteresis band by suitably selecting the switching states of the converter. Hence, DITC controller minimizes the torque ripples and also provides fast response to the torque changes. The performance of DITC controlled SRM drive is analyzed through simulations during acceleration and also in steady state for two types of load torques namely fan type and constant torque. The variation of the switching frequency of the converter is analyzed by changing the torque hysteresis band. It has been observed that as the hysteresis band decreases, the switching frequency increases. So, the hysteresis band cannot be increased beyond a certain limit so as to ensure that the switching frequency of the device cannot increase beyond its operating limit.

Keywords: direct instantaneous torque control, switched reluctance motor, torque ripples

1. Introduction

Switched reluctance motors (SRMs) are replacing the conventional motors in specific applications during last decade due to developments in power electronics and microelectronics

technology. Due to its simple mechanical structure, manufacturing process becomes easy and the cost of the motor becomes low. The rotor is made up of stacks of iron and does not carry any windings or magnets. Thus, it is mechanically robust and naturally suited for high-speed operation. The rotor has the low moment of inertia and high torque/inertia ratio. The SRM achieves high-torque levels at low-peak currents by using small air gaps. The major sources of heat are on the stator, so simple cooling methods can be adopted, as the stator is easier to access than the rotor. The rotor losses are much smaller than the stator as compared to DC, induction and PM machines. As the motor does not produce cogging or crawling torque, skewing is not required to decrease them unlike the induction and PM machines [1–4].

The SRM is a highly reliable motor, as it can function even under faulty conditions with reduced performance. In addition, the motor windings are both physically and electromagnetically isolated from one another, reducing the possibility of phase-to-phase faults. As the windings are electrically separate from each other and as they have negligible mutual coupling, electrical fault in one phase does not affect other phases. Such a feature is unique to the switched reluctance motor. The classic SRM drive as a system with converter involves two switches and a winding in series. Thus, even in case of both switches being turned on simultaneously, no shoot-through faults would occur, unlike the case of AC drives, which lead to shorting of the DC bus [3]. This assures high reliability for this converter compared to other converters. Unidirectional current required by the motor drive makes power electronics drive circuitry simple and reliable.

Main drawback of the motor is that the torque ripples are high as compared to DC and AC machines. Developments in semiconductor technology and microelectronics have resulted in development of sophisticated control strategies to minimize the torque ripples. This has brought the SRM back into the variable-speed drive market. To compete for applications requiring no position sensor, advanced sensor-less techniques have been suggested by the researchers [4]. Applications of the SRM drives are categorized as low, medium, high-power, and high-speed drives [3, 5]. The low-power (less than 3 HP) applications are plotter drive, washing machines, hand-held tools, sliding doors and household appliances (mixer machines, vacuum cleaners with a power range of 0.5–2 kW). The applications in medium power range (less than 300 kW) are industrial general purpose drives, electric vehicles, trains, mining industry; speed applications are textile processing industry, centrifuge for medical applications and aerospace applications [5].

2. Switched reluctance motor

The switched reluctance motor is a doubly salient and singly excited motor. This means that it has salient poles on both stator and rotor as shown in **Figure 1**. The stator poles carry the concentric coils. The diametrically opposite coils on the stator poles are connected to form the phase winding. The rotor has no windings and is built up from a stack of salient pole laminations [6]. The motor operates on the well-known principle of minimum reluctance. When a particular phase is excited, the nearest rotor pole tries to align along the corresponding stator pole axis, so as to minimize the reluctance of the magnetic path. Hence, by sequential
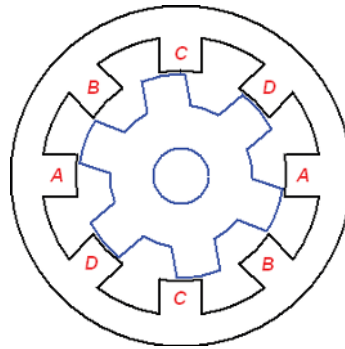
Figure 1. A typical four phase 8/6 SRM.

excitation, the motor can rotate in either direction. An exciting sequence of A-B-C-D for the motor shown in **Figure 1** will result in counter clockwise rotation, while an exciting sequence of C-B-A-D will result in clockwise rotation of the motor [6]. During the rotation, there are three relative positions between the stator and the rotor. When any pair of the rotor poles is exactly aligned with stator poles of a particular phase, that position is called as *aligned position*. Similarly, if the inter-polar axis of the rotor is aligned with the stator poles of a particular phase, that position is called as *unaligned position*. The position between the *aligned* and *unaligned position* is called the *misaligned position* [7].

The mathematical equations of DITC [8, 9] as applied to SRM are discussed here. The instantaneous voltage across the motor winding is given by:

$$v = Ri + \frac{d\psi(\theta, i)}{dt} \tag{1}$$

where $\psi(\theta, i)$ is the phase flux-linkage, which is a function of rotor position θ and current i.

Thus, the equation for the power flow can be written as:

$$vi = Ri^2 + i\frac{\partial\psi(\theta, i)}{\partial i}\frac{di}{dt} + i\frac{\partial\psi(\theta, i)}{\partial\theta}\frac{d\theta}{dt} \tag{2}$$

$$dW_{\mathrm{m}} = i\frac{\partial\psi(\theta, i)}{\partial\theta}d\theta - \frac{\partial W_{\mathrm{f}}}{\partial\theta}d\theta \tag{3}$$

where, dW_{m} and dW_{f} are the differential mechanical energy and field energy, respectively.

The instantaneous torque is defined by:

$$T = \frac{dW_{\mathrm{m}}}{d\theta} \tag{4}$$

The expression for the instantaneous torque production of an SRM phase can be written as:

$$T = i\frac{\partial\psi(\theta, i)}{\partial\theta} - \frac{\partial W_f}{\partial\theta} \tag{5}$$

This is a rarely used variant of conventional torque equation. Due to saturation in the SRM, the influence of the second term in Eq. (5) is negligible. Therefore, by using this approximation, the following equation for torque production may be obtained as:

$$T \approx i\frac{\partial\psi(\theta, i)}{\partial\theta} \tag{6}$$

3. Principle of direct instantaneous torque control

Direct instantaneous torque control strategy as shown in **Figure 2** can be explained as follows [10–13]. The reference torque is compared with the actual torque and given to a hysteresis torque controller, which outputs in torque increase or decrease signal. The output of the torque hysteresis is given to switching control unit. Switching control unit does the following operations: it detects the outgoing and incoming phases based on the position sensor signal, turn-on and turn-off angles of the converter. Next states of both incoming and outgoing phases are determined on the information obtained from instantaneous torque, command torque, and present states of incoming and outgoing phases so as to control the torque within its set band. The asymmetrical converter used to excite the phases of the motor has three possible switching *States*, i.e., 1, 0, and −1 [11, 14].

In single-phase conduction, any one phase is excited, and the total torque is developed by that phase only. If the torque is less than the reference torque, the controller selects *State* as 1 and if it is more than the reference torque *State* is made to −1. *State 0* is not used in this scheme. During phase commutation, two phases conduct simultaneously, and the torque of the two consecutive phases is controlled to control the total torque. The torque is maintained within
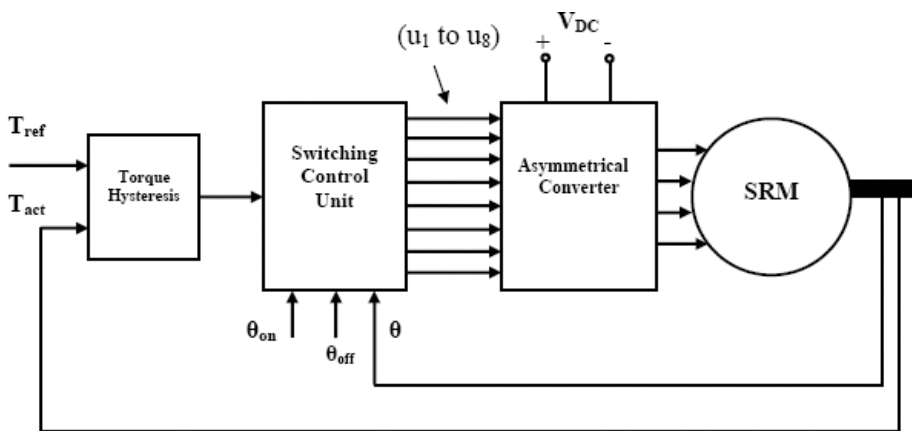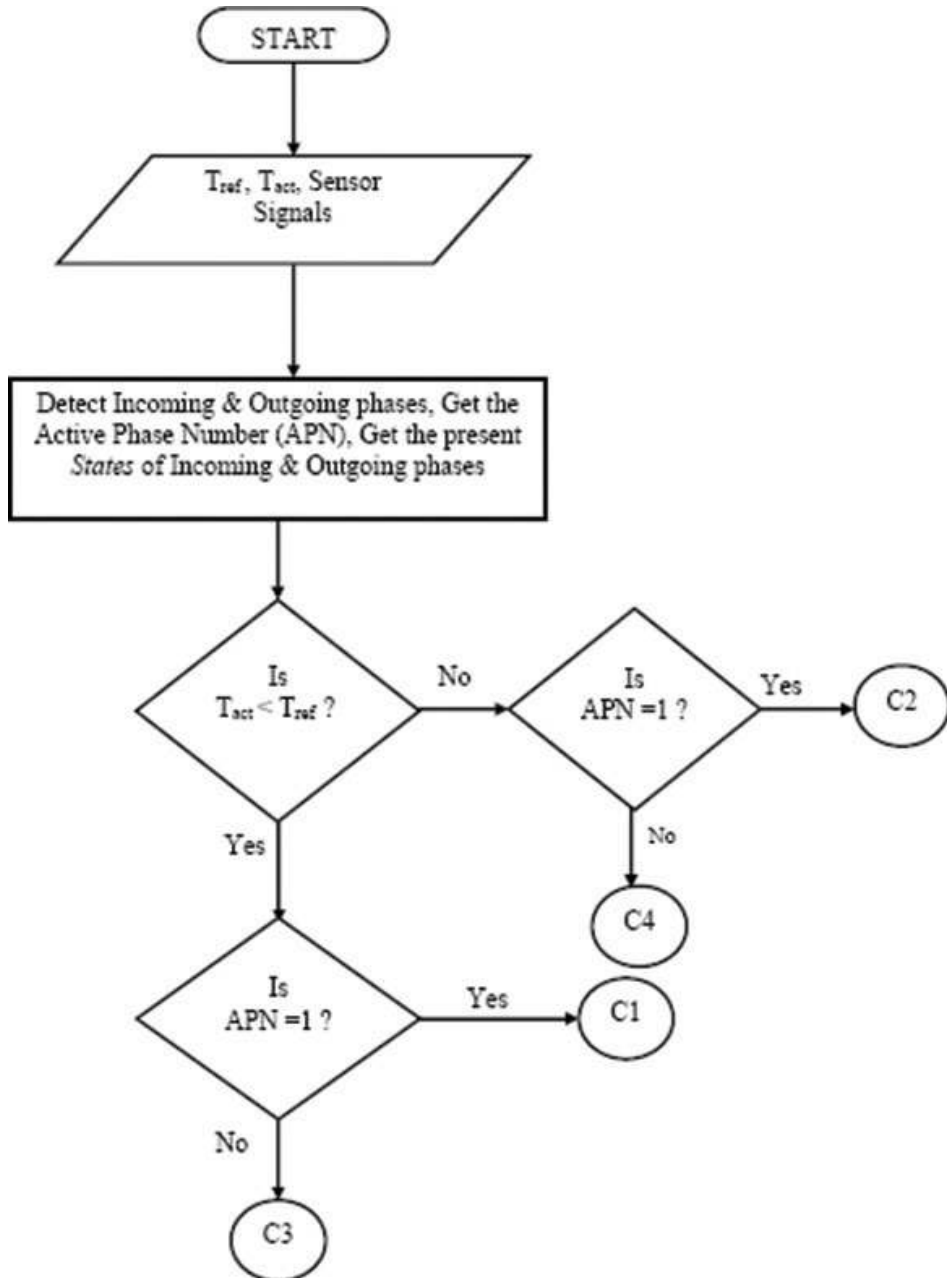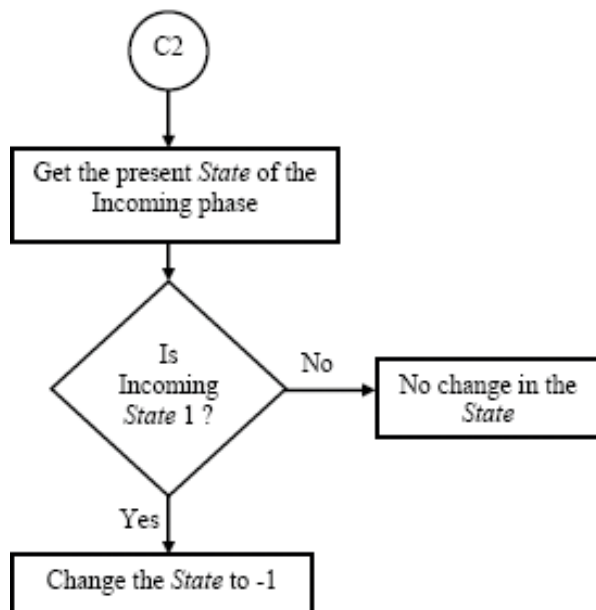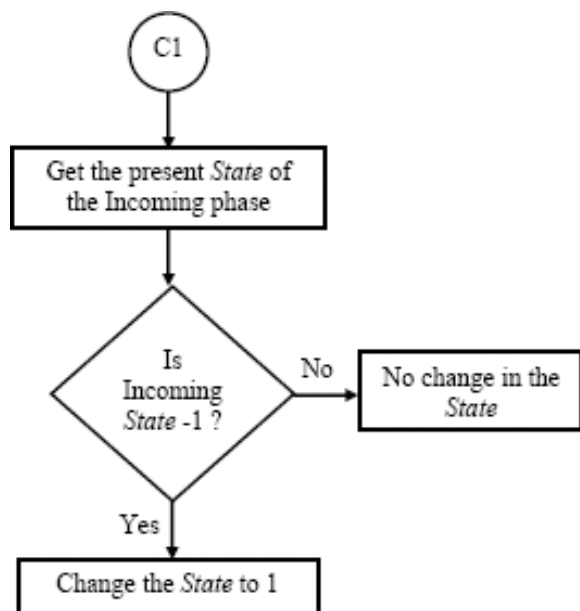

Figure 2. Block diagram of DITC.

hysteresis band, by changing the *States* of the outgoing and incoming phases between 1 and −1, depending on the value of instantaneous torque [11, 14]. The flow chart of the DITC is shown in **Figure 3**.
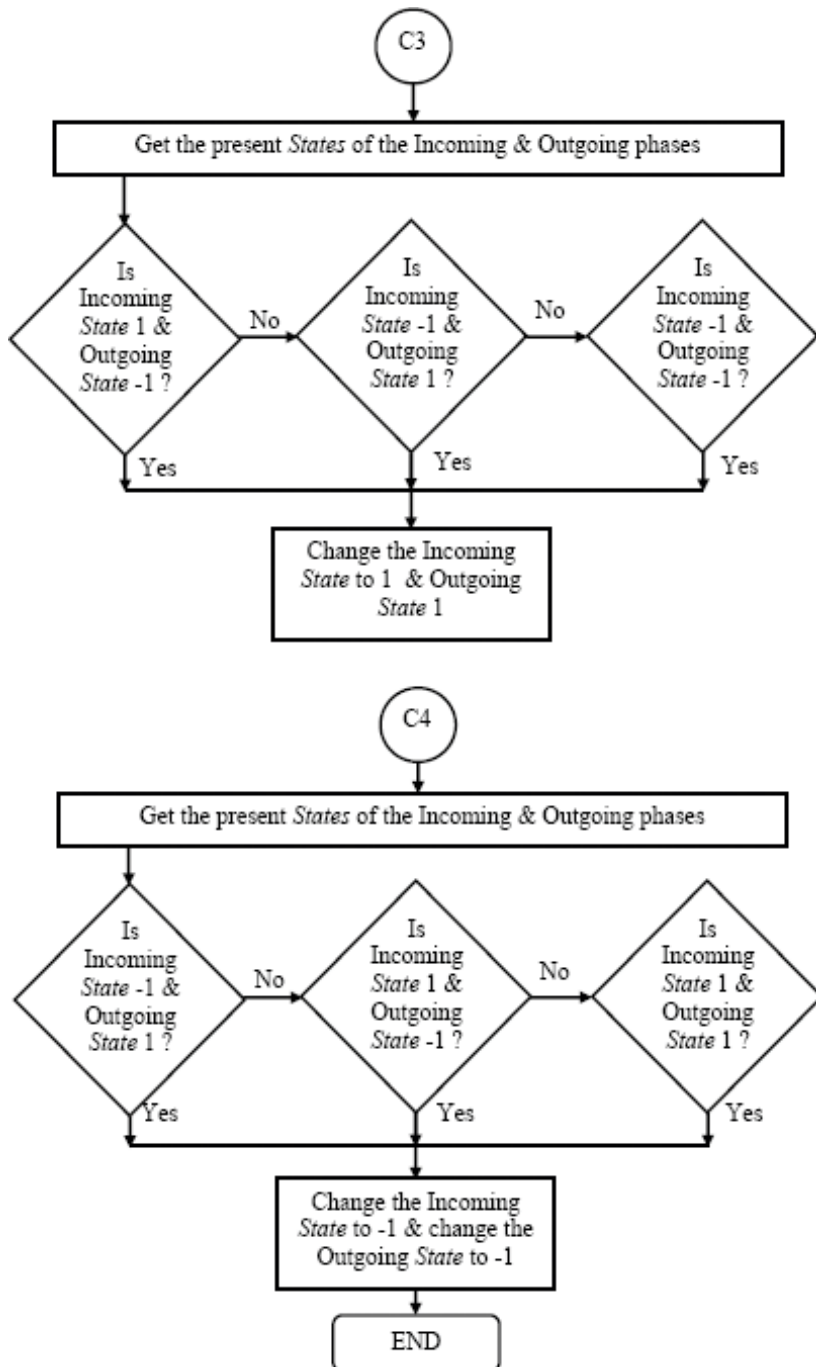
(C1)

Get the present *State* of
the Incoming phase

Is
Incoming
State -1 ?

No → No change in the *State*

Yes

Change the *State* to 1

(C2)

Get the present *State* of the
Incoming phase

Is
Incoming
State 1 ?

No → No change in the *State*

Yes

Change the *State* to -1

Figure 3. (a–d) Flow chart of DITC.

4. Simulation and analysis of DITC

The complete model of the four-phase 8/6 SRM with DITC controller is shown in **Figure 4(a)**. The specifications of the SRM are given in Appendix A. The model consists of electrical system, mechanical system, position sensing, asymmetrical converter, and DITC controller blocks. DITC program is written in the embedded function blocks described in **Figure 3**. **Figure 4(b)** shows the internal model of SRM. The performance of the DITC-based SRM drive is analyzed for a fan-type load of 8 Nm and at a reference speed of 800 rpm. The change in the switching frequency of the device with change in hysteresis band is shown in **Table 1**. The typical frequency of the device is from 5 to 20 kHz. For 5% band of torque hysteresis, the switching frequency is less than 15 kHz, which is the safe operating frequency of the device. Thus, 5% torque hysteresis band can be selected for this drive, because a further decrease in the hysteresis band increases the switching frequency which is beyond the normal operating frequency of the device. It is observed that at lower hysteresis bands, switching frequencies of the device are higher, which increases the switching losses and reduces the efficiency [14].

Total torque of the motor in steady state is shown in **Figure 5(a)**. It is calculated that the torque band is 0.432 Nm as against the set band of 0.40 Nm, while the set band is 0.40 Nm and the torque ripple is 5.41%. **Figure 5(b) (c)** show the voltage applied across two phases, Ph1 and Ph2, respectively. Ph1 is the outgoing phase and Ph2 is the incoming phase. The voltage in each phase changes between +120 and −120 V, in order to maintain total torque same as the load torque. The torque sharing between two consecutive phases is shown in **Figure 5(d)**. During
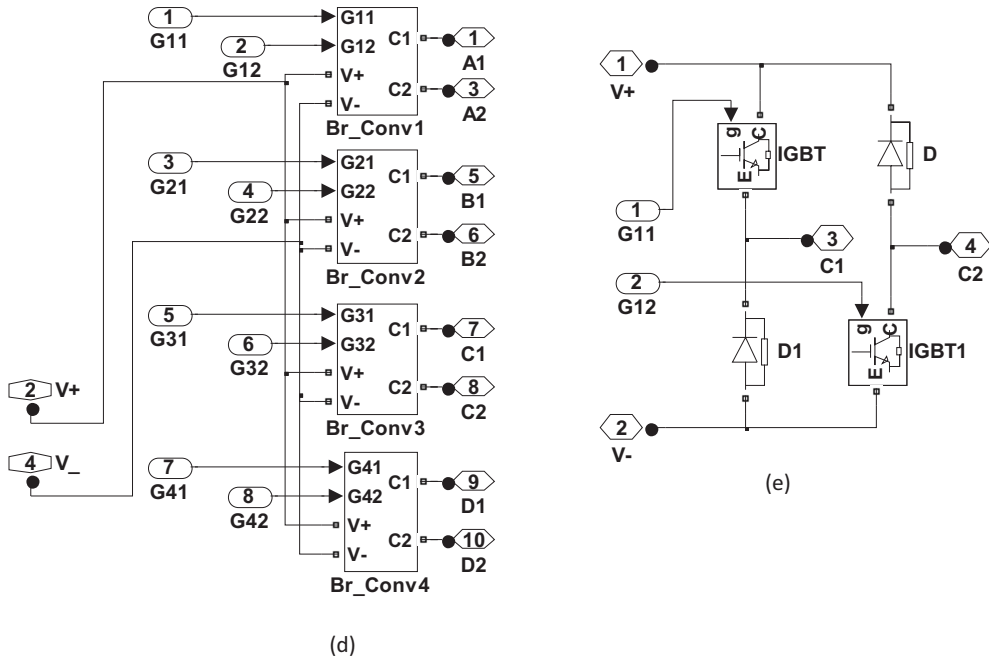

(a)

(b)

(c)

(d)

(e)
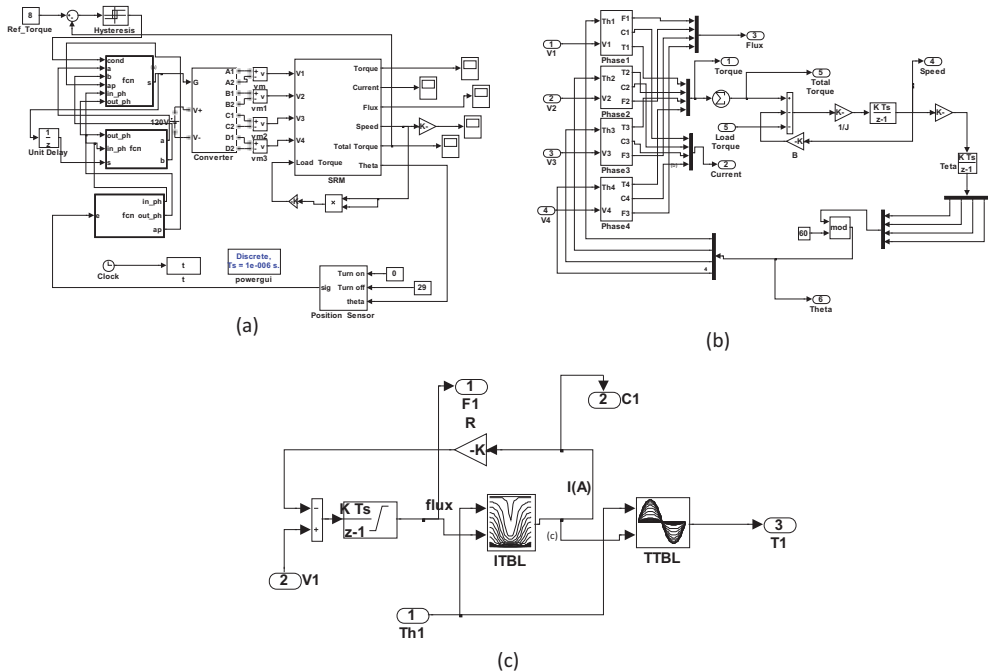
Figure 4. (a) Simulation diagram of SRM drive with DITC, (b) internal block of SRM, (c) internal model of phase 1, (d) asymmetrical converter, and (e) one leg of the converter.

Torque hysteresis band (%)	Switching frequency (f_s) (kHz)
10	6.22
8	8.89
5	13.99
4	16.18
3	21.54

Table 1. Variation of switching frequency with torque hysteresis band.

commutation, it is observed that outgoing torque is decreasing and incoming torque is increasing, but the total torque is kept constant by changing the *States* between 1 and −1. **Figure 6** shows the expanded view of the **Figure 5**.

Torque of all the four phases in the steady state is shown in **Figure 7(a)**, while the current in all the phases is shown in **Figure 7(b)**. The maximum current and average current in each phase are 15.50 and 4.62 A, respectively. **Figure 7(c)** shows the total torque response of the motor. Thus, the torque ripple is minimized in the steady state and during acceleration period. **Figure 7(d)** shows the load torque. **Figure 7(e)** shows the speed response. The steady state speed is maintained constant at 798 rpm. The settling time of the speed is 0.32 s.

The performance of the DITC-based drive is also analyzed for a constant torque load of 8 Nm and at a reference speed of 800 rpm. The simulation diagram is shown in **Figure 8**. The input to the PI controller is the error between the actual speed and the command speed and the output
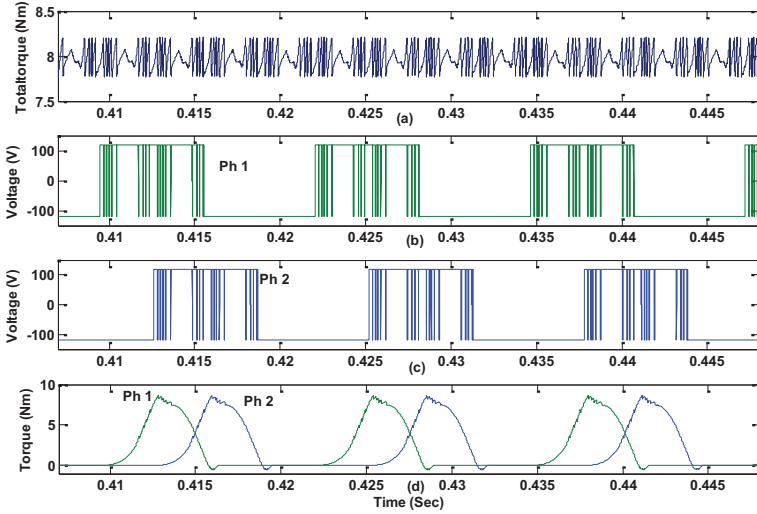
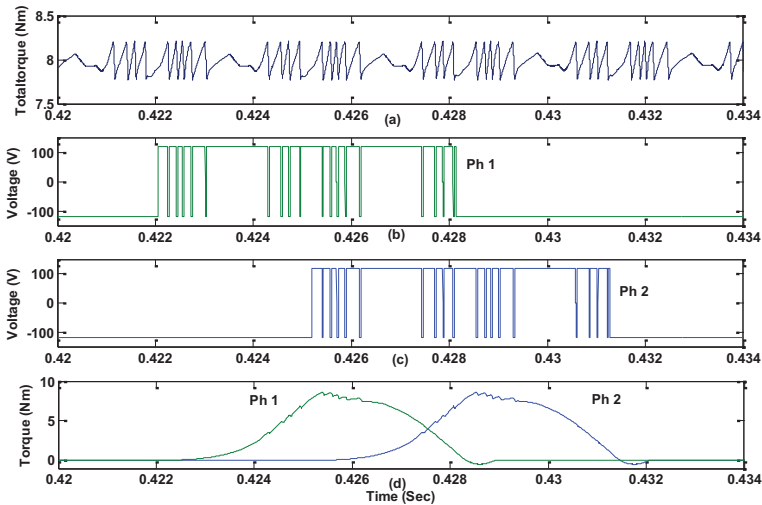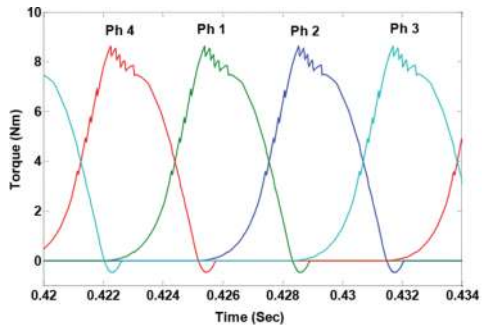**Figure 5.** DITC with fan-type load (a), total torque (b), (c) phase voltages, and (d) phase torques.

Figure 6. Expanded view of Figure 5.
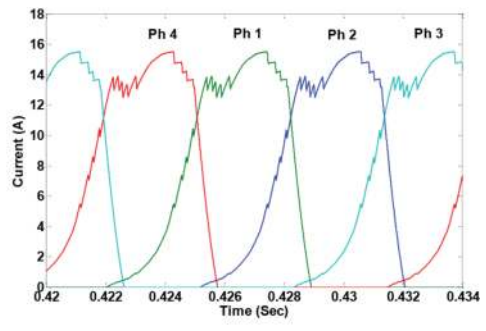
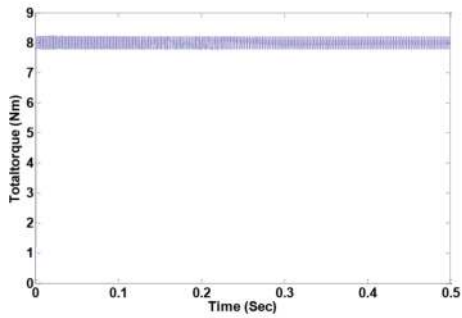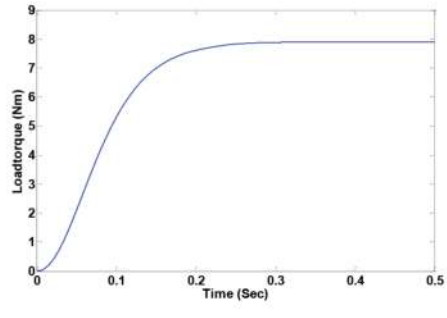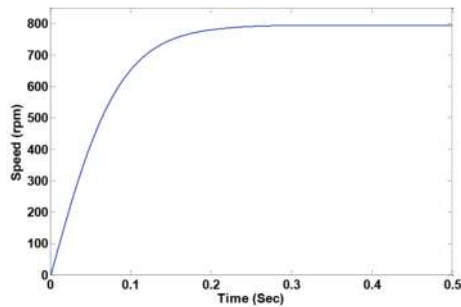**Figure 7.** DITC with fan-type load (a), phase torques (b), phase currents (c), total torque (d), load torque (e) speed.
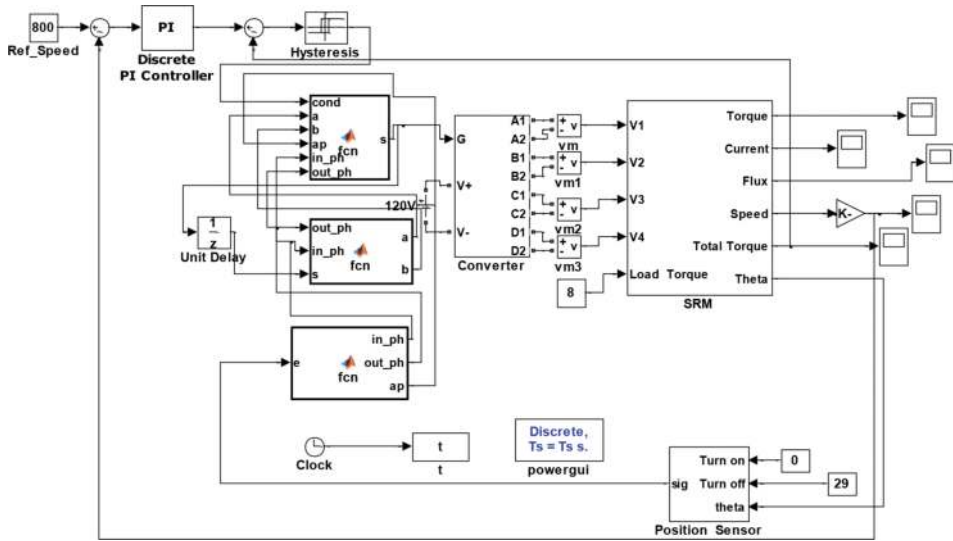
Figure 8. Simulation diagram of SRM drive with direct instantaneous torque controller for constant torque load.
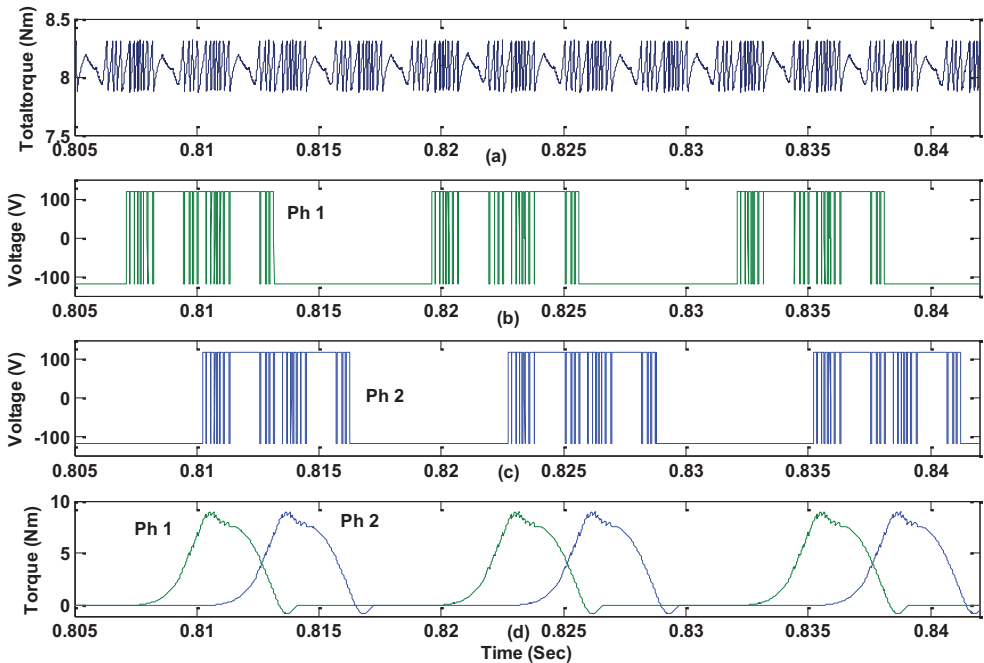

Figure 9. DITC with constant torque load (a), total torque (b), (c) phase voltages, and (d) phase torques.
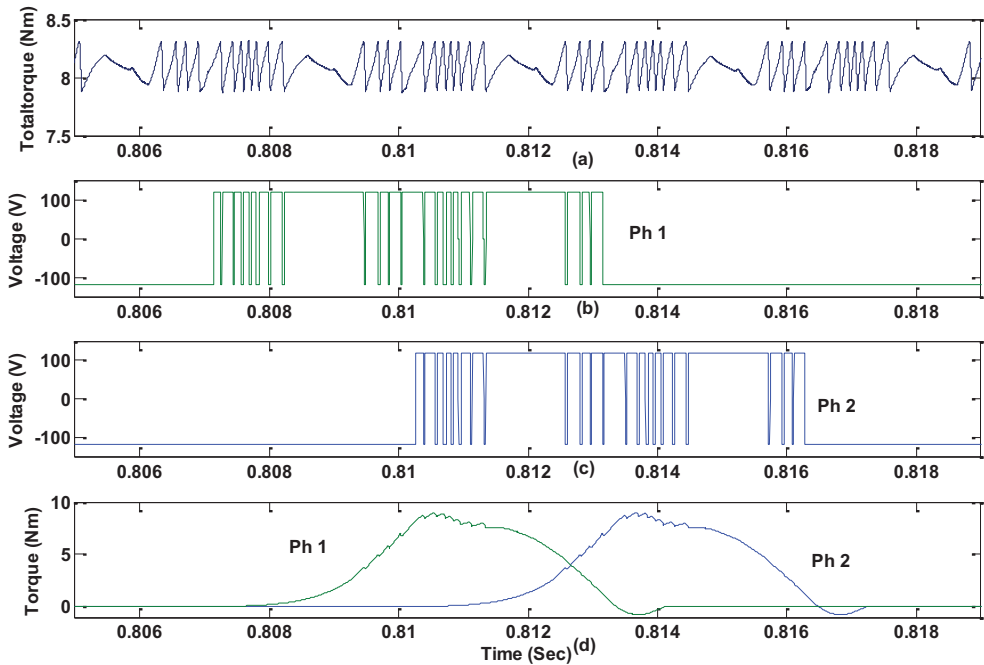
Figure 10. Expanded view of Figure 9.

is the command torque. Whenever the speed is less than the command speed, the output of the PI controller is 9 Nm. The output of PI controller is equal to the load torque when the speed reaches the reference value.

Simulation waveforms of the DITC-based drive for constant torque load are shown from **Figures 9(a)–(d)**, **10**, and **11(a)–(e)**. It is observed that the torque is maintained within a band of 0.43 Nm as against the set band of 0.40 Nm. The torque ripple is only 5.38% in steady state. The maximum current and average current in each phase are 17.59 and 5.00 A, respectively. Thus, the torque ripple is minimized in the steady state and during acceleration period. The settling time of the speed is 0.713 s. The variation of peak current, average current, torque ripple, and speed settling time for DITC-based SRM drive is given in **Table 2**.

From the **Table 2**, it is observed that the peak current, average current, and settling time is higher for constant torque load as compared to fan load. There is no significant variation in the torque ripple for both types of loads. Switched reluctance motor drives with sophisticated direct instantaneous torque control can minimize the torque ripples and increases the efficiency of the drive when operated at the required torque band and thus can be included in the future energy technologies.

(a)

(b)

(c)

(d)

(e)
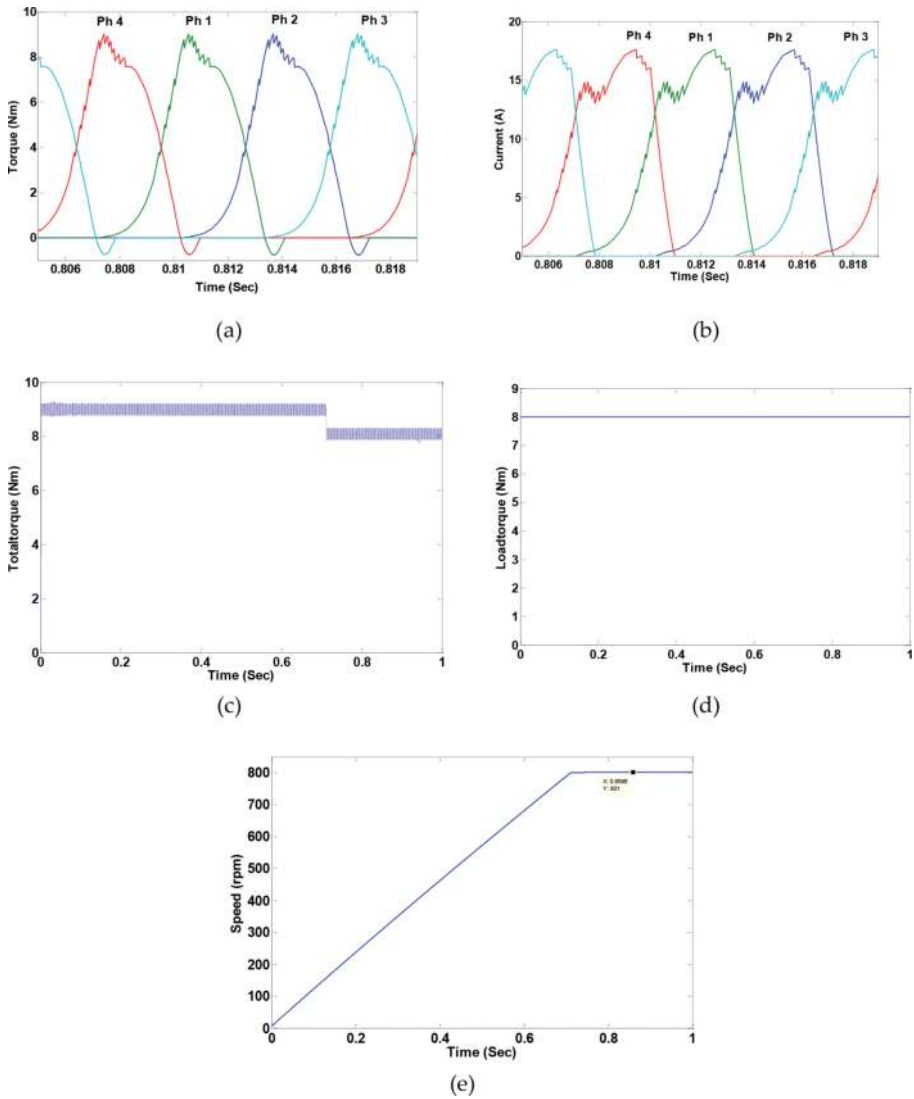
Figure 11. DITC with constant torque load (a), phase torques (b), phase currents (c), total torque (d), and load torque (e) speed.

Type of load	Peak current (A)	Average current (A)	% Torque ripple	Settling time (s)
Fan-type load	15.50	4.62	5.41	0.32
Constant torque load	17.59	5.25	5.38	0.71

Table 2. Comparative analysis for fan-type load and constant torque load with DITC.

5. Conclusion

A more sophisticated control technique named direct instantaneous torque control is presented in this chapter. In this control strategy, the torque is maintained within a set hysteresis band by changing the switching *States* of the phases. The torque ripple variation with switching frequency has been analyzed with DITC controller under accelerating and steady state conditions.

The DITC controlled drive is simulated in MATLAB/SIMULINK environment with fan load and constant torque and is observed that the controller maintains the total torque within its set band during steady state and also while accelerating. The switching frequency under such conditions is 13.99 kHz. Thus, it can be concluded that, unlike conventional techniques, DITC control does not require any current profiles or torque sharing functions.

A comparative analysis of DITC-based drive with constant torque load and fan-type load is made. It is observed that the peak current and average current are higher for constant torque load compared to fan-type load. The torque ripple is almost same for both types of loads. The speed settling time for constant torque load is more than twice the value obtained with fan-type load.

Appendix A

Voltage	120 V DC
Maximum current	30 A
Rated speed	1500 rpm
Maximum flux	0.3 Wb
Aligned inductance	110 mH
Unaligned inductance	10 mH
Resistance	0.3 Ω
Stator poles	8
Rotor poles	6

Author details

Srinivas Pratapgiri

Address all correspondence to: srinivasp.eedou@gmail.com

Department of Electrical Engineering, University College of Engineering, Osmania University, Hyderabad, India

References

[1] Miller TJE. Switched Reluctance Motors and Their Control. Magna Physics Publishing & Oxford University Press; 1993

[2]   Miller TJE. Electronic Control of Switched Reluctance Machines. Oxford & Boston: Newnes Press; 2001

[3]   Krishnan R. Switched Reluctance Motor Drives: Modeling, Simulation, Analysis, Design, and Applications. CRC Press; 2001

[4]   Emadi A. Energy-Efficient Electric Motors. 3rd ed. Marcel Dekker; 2005

[5]   De Doncker R, Pulle DWJ, Veltman A. Advanced Electrical Drives: Analysis, Modeling and Control. Springer; 2011

[6]   Wenzhe Lu. Modeling and control of switched reluctance machines for Electro-Mechanical braking system [thesis]. The Ohio State University; 2005

[7]   Wang X. Modeling and implementation of controller for switched reluctance motor with AC small signal model [thesis]. Virginia Polytechnic Institute and State University; 2001

[8]   Cheok AD, Hoon PH. A new torque control method for switched reluctance motor drives. In: 26th Annual Conference of the IEEE Industrial Electronics Society; 22-28 October 2000; Nagoya, Japan. IEEE; 2000. pp. 387–392

[9]   Cheok AD, Fukuda Y. A new torque and flux control method for switched reluctance motor drives. IEEE Transactions on Power Electronics. 2002;**17**(4):543–557

[10] Inderka RB, De Doncker RW. DITC-Direct instantaneous torque control of switched reluctance drives. IEEE Transactions on Industry Applications. 2003;**39**(4)

[11]   Fuengwarodsakul NH, Menne M, Inderka RB, De Doncker RW. High_dynamic Four-Quadrant switched reluctance drive based on DITC. IEEE Transactions on Industry Applications. 2005;**41**(5)

[12] Chancharoensook P. Direct instantaneous torque control of a Four-Phase switched reluctance motor. In: International Conference on Power Electronics and Drive Systems; 2-5 November 2009; Taipei, Taiwan. IEEE; 2009. pp. 770–777

[13] Inderka RB, Krehenbrink M, De Doncker RW. On-line Estimation of Instantaneous Torque of Switched Reluctance Machines. In: International Symposium on Industrial Electronics; 4-8 December 2000; Cholula, Puebla, Mexico. IEEE; 2000

[14] Srinivas P, Prasad PVN. Torque ripple minimization of 4 phase 8/6 switched reluctance motor drive with direct instantaneous torque control. International Journal on Electrical Engineering and Informatics. 2011;**3**(4):488–497